Atmos. Chem. Phys. Discuss., 11, 32847–32875, 2011
www.atmos-chem-phys-discuss.net/11/32847/2011/
doi:10.5194/acpd-11-32847-2011


Atmospheric Chemistry and Physics Discussions



# Dry deposition fluxes and deposition velocities of seven trace metal species at five sites in Central Taiwan – a summary of surrogate surface measurements and a comparison with model estimation

**L. Zhang[1], G. C. Fang[2], C. K. Liu[2], Y. L. Huang[2], J. H. Huang[2], and C. S. Huang[2]**

[1]Air Quality Research Division, Science and Technology Branch, Environment Canada, 4905 Dufferin St., Toronto, Ontario, M3H5T4, Canada
[2]Department of Safety, Health and Environmental Engineering, HungKuang University, Sha-Lu, Taichung 433, Taiwan

Received: 31 October 2011 – Accepted: 28 November 2011 – Published: 13 December 2011

Correspondence to: L. Zhang (leiming.zhang@ec.gc.ca)
G. C. Fang (gcfang@sunrise.hk.edu.tw)

Published by Copernicus Publications on behalf of the European Geosciences Union.







## Abstract

Daily air concentrations and dry deposition fluxes of seven metal species were monitored at five sites in Central Taiwan for five or six days each month from September 2009 to August 2010. Annual average concentrations at the five sites were in the range of 2.8 to 3.6 ng $m^{-3}$ for As, 25 to 82 ng $m^{-3}$ for Mn, 1900 to 2800 ng $m^{-3}$ for Fe, 69 to 109 ng $m^{-3}$ for Zn, 18 to 33 ng $m^{-3}$ for Cr, 60 to 110 ng $m^{-3}$ for Cu, and 25 to 40 ng $m^{-3}$ for Pb. Annual average dry deposition fluxes were on the order of 3, 20, 400, 50, 25, 50 and 50 µg $m^{-2}$ $day^{-1}$ for As, Mn, Fe, Zn, Cr, Cu and Pb, respectively. Annual average dry deposition velocities ($V_d$) for the seven metal species ranged from 0.18 to 2.22 cm $s^{-1}$ at these locations. Small seasonal and geographical variations, e.g., from a few percent to a factor of 2 for different species and/or at different locations, were found for measured concentrations, fluxes and $V_d$. Measured fluxes and air concentrations had moderate to good correlations for several species at several sites, but had weak or no correlations for other species or at other sites, the latter cases were believed to have large uncertainties in flux measurements using surrogate surfaces. Sensitivity tests were conducted for particle $V_d$ using a size-segregated particle dry deposition model, assuming various combinations of three lognormal size distributions representing fine particles ($PM_{2.5}$), coarse particles ($PM_{2.5-10}$) and super size particles ($PM_{10+}$), respectively. It was found that measured dry deposition fluxes can be reproduced reasonably well using the size-segregated particle dry deposition model if the mass fractions of metal species in $PM_{2.5}$, $PM_{2.5-10}$ and $PM_{10+}$ were known. Significant correlations between modeled and measured daily fluxes were found for those cases that were believed to have small uncertainties in flux measurements.

## 1 Introduction

Air pollutants can be harmful to human health by the following pathways: (1) they may be absorbed into human lung tissues during breathing, and (2) they can dry and wet





ACPD
11, 32847–32875, 2011



deposit into various terrestrial and aquatic ecosystems and cause subsequent health effects when the products from these ecosystems are consumed by humans. Quantifying the amount of dry and wet deposition is critical since these deposition processes determine pollutant species' lifetime in air and their input to various ecosystems. Due to the expensive cost and technical difficulties in the direct measurements of dry deposition, the inferential method has been commonly used to estimate dry deposition, especially at multiple locations or at regional to global scales. Several recent studies suggested that uncertainties in dry deposition estimates are on the order of a factor of 2 on annual basis for several commonly studied sulfur and nitrogen species and ozone (Flechard et al., 2011; Schwede et al., 2011). The uncertainties could be larger for particle species than for gaseous species due to the strong dependence of particle dry deposition velocity ($V_d$) on particle size (Petroff and Zhang, 2010).

Many trace metals are toxic to humans and ecosystems and their input to surface waters and terrestrial environment need to be quantified (Rojas et al., 1993; Pirrone et al., 1995; Odabasi et al., 2002; Lu et al., 2003; Koçak et al., 2005; Sabin et al., 2006; Tasdemir et al., 2006; de P. Pereira et al., 2007; Sakata et al., 2006, 2008; Al-Momani et al., 2008). Field studies measuring metal dry deposition are limited and $V_d$ generated from these studies differ from each other significantly (Migon et al., 1997; Sakata and Marumoto, 2004; Tasdemir and Kural, 2005; Wu et al., 2006; Yi et al., 2001, 2006; Fang et al., 2004, 2007a,b). The differences in measured $V_d$ were likely caused by different meteorological conditions, different particle size distributions, and measurement uncertainties. The majority of existing dry deposition measurements for trace metals made use of surrogate surfaces which might not represent natural surface conditions.

The main purpose of the present study is to summarize the measured dry deposition fluxes and deposition velocities of seven metal species (As, Mn, Fe, Zn, Cr, Cu, Pb) collected at five sites in Central Taiwan and to investigate if the measured deposition flux and velocities can be reproduced by a commonly used dry deposition model of Zhang et al. (2001). It is expected that the comparison between measurements and





ACPD
11, 32847–32875, 2011



model estimations can shed some light on the possible uncertainties in both measurements and modeling approaches. Brief discussion of the geographical and seasonal patterns of measured air concentration is also presented since dry deposition fluxes are closely linked to the air concentrations.

## 2 Measurements

### 2.1 Brief description of field experiments

Daily air concentrations and fluxes for seven metal species (As, Mn, Fe, Zn, Cr, Cu and Pb) were collected at five sampling sites in Central Taiwan for five or six days in each month during one year period (September 2009 to August 2010). The locations of the five sampling sites are shown in Fig. 1. Although the five sites are all located in a small region (within several hundred square kilometers) in Central Taiwan, each site has its own characteristics and local emission sources. Briefly, Site I (Bei-shi) is a coastal suburban site with fossil fuel combustion and transportation as major emission sources; Site II (Chang-hua) is an urban center site with transportation, chemical plant and fossil fuel combustion as major emission sources; Site III (He-mei) is a residential site with emissions from transportation, fossil fuel combustion, heating and waste incineration; Site IV (Quan-xing) is an industrial site with emissions from steel industry, electronic industry, plastic industry, chemical industry, basic metal manufacturing, machinery manufacturing, petroleum and coal products; and Site V (Gao-mei) is a wetland site (mostly agricultural land) with emissions from a nearby Taichung thermal power plant and fossil fuel combustion.

Total suspended particulate matter (TSP) was collected using PS-1 instruments (GPS1 Polyurethane Foam (PUF) Sampler, General Metal Work). The maximum size of collected particles was $\sim 100\,\mu m$. Dry deposition fluxes were collected using a surrogate surface made of polyvinyl chloride. More information on the instrument, the chemical analysis procedure and data quality control is provided in the document of





ACPD
11, 32847–32875, 2011



Supporting Information. Some descriptions can also be found in Fang et al. (2007a,b).

## 2.2 Air concentrations

Annual average concentrations at the five sites were in the range of 2.8 to 3.6 ng $m^{-3}$ for As, 25 to 82 ng $m^{-3}$ for Mn, 1900 to 2800 ng $m^{-3}$ for Fe, 69 to 109 ng $m^{-3}$ for Zn, 18 to 33 ng $m^{-3}$ for Cr, 60 to 110 ng $m^{-3}$ for Cu, and 25 to 40 ng $m^{-3}$ for Pb (Table 1). Geographical variations in the annual average concentrations were smallest for As (< 30 %), in the range of 45–80 % for Fe, Zn, Cr, Cu and Pb, and largest for Mn (a factor of 3). Site V had the lowest annual concentrations for all the metal species monitored. This is because the site was a wetland site and thus both anthropogenic sources and crustal sources were lowest among all the sites. Site IV had the highest annual concentrations for most metal species (except Cr) due to the heavily industrialized areas. Concentrations of As, Fe, Zn, Cr at the urban center (Site II) were similar (within a range of 10 %) to those at the industrial center (Site IV), but the other three metals species (Mn, Cu and Pb) were 30 % smaller than those at Site IV.

It is known that metal smelting is one main source for Fe, Mn and Pb; coal combustion is one main source for Cr; vehicle exhaust is one main source for Cr, Pb, Cu, Zn and Fe; incinerator is one main source for Zn; soils and re-suspended are also main sources for Fe and Mn (Chao and Wong, 2002; Loska and Wiechuła, 2003; Funasaka et al., 2003; Singh et al., 2005; Akhlaghi and Kompany-Zareh, 2005; Kim et al., 2006; Napier et al., 2008; Wu et al., 2010). The geographical differences for different metal species discussed above were certainly caused by their different (anthropogenic and natural) sources. For example, the Mn concentrations were much higher at the industrial site than at the rest of the sites, while the Cr concentrations were basically the same at the urban center and the industrial sites.

Seasonal variations of the averaged concentrations were generally consistent from site to site, but different for different metal species (Fig. 2). Most metal species at the majority of the sites had lowest concentrations in summer; Mn, Fe and Zn had highest concentrations in winter, Cr had highest concentrations in spring; and Pb had highest





ACPD
11, 32847–32875, 2011



concentrations in fall. Seasonal variations for some species during several seasons were small (within a few ten percent) due to the small changes in meteorological conditions in this region (Table S1). Information on anthropogenic emission inventory and size-distribution (or fine and coarse fractions) of each metal specie are needed in order to identify the causes of different seasonal patterns. Concentrations for the seven species obtained in the present study were on similar order of magnitude to several studies conducted in other parts of the world, noting that the differences in concentrations among the existing studies could be more than one order of magnitude (Odabasi et al., 2002 and references therein).

### 2.3 Dry deposition fluxes

Average dry deposition fluxes were on the order of 3, 20, 400, 50, 25, 50 and 50 $\mu g\,m^{-2}\,day^{-1}$ for As, Mn, Fe, Zn, Cr, Cu and Pb, respectively, at the five sites. The geographical variations in fluxes were within 30 % for As, Mn, Fe, Zn and Cr but were up to 50 % for Cu and Pb. These flux variations were smaller than those for concentrations discussed above. One major reason causing the reduced geographical variation in fluxes compared to those in concentrations was that the highest deposition velocities were observed at Site V which had the lowest concentrations (more discussion below). Annual fluxes obtained in the present study were well in the range of previous studies around the world, e.g., 6 to 135 $\mu g\,m^{-2}\,day^{-1}$ for Mn, 240 to 12 090 $\mu g\,m^{-2}\,day^{-1}$ for Fe, 9 to 1910 $\mu g\,m^{-2}\,day^{-1}$ for Zn, 1 to 53 $\mu g\,m^{-2}\,day^{-1}$ for Cr, 3 to 190 $\mu g\,m^{-2}\,day^{-1}$ for Cu, and 5 to 220 $\mu g\,m^{-2}\,day^{-1}$ for Pb (Tasdemir and Kural, 2005 and references therein).

Seasonal variations of the fluxes (Fig. S1) had patterns similar to those of concentrations for most cases, but some differences were also found. For example, significantly higher fluxes in the fall were found for Cu at Sites II to V, but not in the concentrations. For most metal species (except Cu and Pb), seasonal variations of fluxes were smaller than those of concentrations at Sites I to IV, but the opposite was found at Site V. Again, this was caused by the much higher deposition velocities found at Site V compared to





ACPD
11, 32847–32875, 2011



the other sites.

### 2.4 Dry deposition velocities

Daily dry deposition velocities ($V_d$) were obtained from the ratio of measured daily fluxes and concentrations and were then averaged into annual (Table 1) and seasonal (Fig. S2) values. Annual average $V_d$ at the five sites ranged from 0.97 to 1.08 cm s$^{-1}$ for As, 0.37 to 0.98 cm s$^{-1}$ for Mn, 0.18 to 0.26 cm s$^{-1}$ for Fe, 0.56 to 0.85 cm s$^{-1}$ for Zn, 0.93 to 1.60 cm s$^{-1}$ for Cr, 0.78 to 0.88 cm s$^{-1}$ for Cu, and 1.88 to 2.22 cm s$^{-1}$ for Pb. While $V_d$ for a few metal species only changed slightly from site to site, $V_d$ for other species changed significantly (e.g., a factor of 2). Since all five sites were located within a few hundred square kilometres, meteorological conditions only differed slightly from site to site (Table S1). This explains the small differences in $V_d$ from site to site for a few metal species (e.g., As, Fe, Cu). The very large difference in $V_d$ from site to site for a few species (e.g., Mn, Cr) should thus be caused by their different size distributions at different sites considering the strong dependence of $V_d$ on particle size distribution (more discussion in Sect. 3).

Seasonal variations of $V_d$ were small (e.g., 10 % or less) for many species and at most sites. This again can be explained by the small seasonal differences in meteorological conditions since all the sites were located in a tropical region. However, seasonal variations as large as a factor of 2 were found for Cu at Site II and for Pb at Sites II, III and V. Size distributions of particles should be the major causes as explained above. Flux measurement uncertainties for these two species were also suspected to be larger than for other species as discussed in Sect. 2.5. It is also noticed that $V_d$ values of Fe were much smaller than those of Pb in this study. This was consistent with one of our earlier studies (Fang et al., 2007a), but contrary to a few other of our earlier studies (Fang et al., 2004, 2007b), all of which were conducted using the same instruments but at different locations in Taiwan. Different size distributions at different locations (especially the mass fraction of particles larger than 10 µm as discussed in Sect. 3) was suspected to be the major causes of the large differences in the $V_d$ of Fe.





ACPD
11, 32847–32875, 2011



The annual average $V_d$ for the seven metal species obtained in the present study (0.18 to 2.22 cm s$^{-1}$) were in the range of previous field studies on trace metals. For example, Yi et al. (2001) obtained $V_d$ ranged from 0.2 to 12 cm s$^{-1}$ for various crustal and anthropogenic elements; Odabasi et al. (2002) obtained $V_d$ of 1.0–6.2 for various metal species (including all species studied here except As). On the other hand, Tasdemir and Kural (2005) obtained $V_d$ of 2.3 to 11.1 cm s$^{-1}$ for 13 trace elements and their values were all higher than values presented in this study. Apparently, large differences existed in $V_d$ from different studies and were most probably caused by a combination of different particle size distribution, different meteorological conditions and measurement uncertainties. It should be noted here that $V_d$ to the natural surface could differ significantly from those to the surrogate surfaces used in these studies.

### 2.5 Correlation between measured fluxes and concentrations

The dry deposition fluxes of a pollutant strongly depend on its air concentrations. Thus, theoretically, measured fluxes and concentrations should be correlated significantly (e.g., Yi et al., 2006). However, due to the measurement uncertainties, especially in the flux measurements using surrogate surfaces, the correlation between measured fluxes and concentrations might not be satisfactory. Figure 3 shows the flux-concentration regression equations for Mn at the five sites as an example and the same information for the other six metal species are shown in Fig. S3. The square of correlation coefficient ($R^2$) ranged from 0.34 to 0.58 for Mn at Sites II to V, suggesting that the fluxes and concentrations were moderately correlated. This provides some confidence on the measured fluxes using surrogate surfaces. However, the correlation between fluxes and concentrations for Mn at Site I was extremely low, which might imply large measurement uncertainties in fluxes at this site.

Looking at the other six species, almost no correlation between fluxes and concentrations was found for Cu at all the sites; low to moderate correlations were found for As, Cr and Pb at most sites; and moderate to good correlations were found for Fe and Zn at most sites. While variations in meteorological conditions and particle size





ACPD
11, 32847–32875, 2011



distributions caused variations in deposition velocities which in turn led to the low correlation between measured fluxes and concentrations, measurement uncertainties in concentrations and especially in surrogate-surface fluxes should have played a major role. This assumption seems to be confirmed when compared with the much improved correlations between modeled fluxes and measured concentrations discussed below.

## 3 Model estimates

### 3.1 Brief review of size distributions of metal species

Due to the strong dependence of the dry deposition velocity ($V_d$) on particle size, knowledge of particle size distribution (PSD) is extremely important in particle dry deposition studies. Measurements of PSD were limited for many metal species. A detailed review of PSD of Pb-containing atmospheric particles was recently conducted by Cho et al. (2011). PSD for several other metals were briefly reviewed here so the information can be used for modeling their dry deposition and for other air pollution studies.

PSD data collected at three background sites in UK showed three types of PSD: (1) A major mode at ~ 0.5 µm and additional minor modes at 1.2 and 6.0 µm or at 3.5 and 20 µm, depending on locations, for Cd, Sn, Pb and Se; (2) multiple modes throughout the size range and more evenly distributed mass for Ni, Zn, Cu, Co, Mn and Hg; (3) a large mode at ~ 3–4 µm for Fe, Sr, and Ba (Allen et al., 2001). The same study also showed that particles larger than 10 µm could contribute 10–20 % to the total mass for several species considered in the present study (e.g., Mn, Fe, Zn, Cu). PSD measured in a residential area (Kyoto, Japan) showed a typical bimodal distribution with S, Zn and Pb found predominantly in fine particles (peaked at 0.5–1 µm), Si, Ca, Fe and Ti found predominantly in coarse particles (peaked at ~ 5 µm), and K, V, Cr, Mn, Ni, Cu and Br evenly distributed in both fine and coarse fractions (peaked at 0.5–1 and 5 µm) (Kasahara et al., 1996). Both unimodal (either in fine or coarse particles) and bimodal (one fine and one coarse) PSD were found in an urban environment (Brüggemann





ACPD
11, 32847–32875, 2011



et al., 2009).

Size-fractionated data were conducted in several studies, although PSD profiles were not generated (e.g., Monarca et al., 1997; Singh et al., 2002; Turšič et al., 2006; Wang et al., 2006; Yi et al., 2006; Karanasiou et al., 2007). A few studies investigated mass fractions of the commonly defined size ranges (e.g., $PM_{1.0}$, $PM_{2.5}$, $PM_{10}$) (Zota et al., 2009; Makkonen et al., 2010). These studies suggested that fine particles dominated the total mass in some cases (species or locations) while coarse particles dominated the total mass in other cases. One study investigated the fraction of $PM_{10}$ in TSP (de Pereira et al., 2007) and showed that particles larger than 10 µm could contribute a few ten percent to TSP mass at some locations.

Mass median diameter (MMD) from the data collected at an urban site in Japan (Tokyo) were in the range of 0.92 to 1.4 µm for Cd, 1.0–1.5 µm for Pb, 1.2 to 2.0 µm for Zn, 2.9 to 3.9 µm for Cu and 2.5 to 4.1 µm for Mn (Sakata and Marumoto, 2004). In another study conducted in an urban environment (at a roadside) the MMD data was Pb (0.91) < Cd(1.14) < V(1.38) < Ni(1.54) < Cu(2.04) < Mn(2.61) < Cr(2.91) < Fe(3.82) (Samara and Voutsa, 2005). Knowledge related to the size distributions discussed above was used below for estimating $V_d$ for the seven metal species.

### 3.2 Modeled dry deposition velocities

Literature review presented in Sect. 3.1 suggested that most metal species have more than one mode in their size distributions. For the seven species considered in the present study, fine and coarse particles are both important to the total mass. Particles larger than > 10 µm could also contribute a few percent to 20 % of the total mass.

To model $V_d$ as accurately as possible, a full size distribution is needed as suggested in several previous studies (Holsen and Noll, 1992; Paode et al., 1998; Sofuoglu et al., 1998). In the present study, three log-normal size distributions representing fine mode ($PM_{2.5}$) (referred to size 1 in Table 2), coarse mode ($PM_{2.5-10}$) (referred to size 2) and large mode ($PM_{10+}$) (referred to size 3), respectively, are first assumed. The geometric mass median diameter and geometric standard deviation chosen are 0.45 µm and 2.0,





ACPD
11, 32847–32875, 2011



respectively, for size 1, 4.5 µm and 1.6 for size 2, and 20 µm and 1.6 for size 3 (see their size distributions in Fig. S4). Size-segregated $V_d$ is calculated using the model of Zhang et al. (2001) with modifications on the handling of seasonal-dependent input parameters (Zhang et al., 2003) (see SI for a brief description of the model). The size-segregated $V_d$ is then averaged into bulk $V_d$ based on the size distributions for each of the size 1, size 2 and size 3. Different combinations of these three modes, which could represent different metal species' size distributions, are then designed to see how sensitive the bulk $V_d$ is to the size distributions (size 4 to size 10 listed in Table 2). Daily meteorological data (wind speed, relative humidity, and temperature) were obtained from nearby meteorological stations and were used in $V_d$ calculations.

Modeled annual average $V_d$ at the five sites ranged from 0.09 to 0.19 cm s$^{-1}$ for size 1, from 0.20 to 0.22 cm s$^{-1}$ for size 2, and from 3.75 to 4.58 cm s$^{-1}$ for size 3. Different meteorological conditions and underlying surface types among the five sites caused a factor of 2 difference in the modeled $V_d$ of size 1, but only caused a small difference (e.g., ~20 % or less) in those of size 3 and almost no differences in those of size 2. While $V_d$ of size 2 were slightly higher (by 10 % to a factor of 2) than those of size 1, $V_d$ of size 3 were more than one order of magnitude higher than those of size 1 and size 2.

Due to the small $V_d$ values for both size 1 and size 2, $V_d$ for various combinations of size 1 and size 2 (e.g., Sizes 4–6 in Tables 2 and 3) were all smaller than 0.22 cm s$^{-1}$ at all the sites. Assuming 10 % of total mass were from particles larger than 10 µm ($PM_{10+}$) (e.g., size 7 and size 8), the bulk $V_d$ for TSP could then be increased to 0.46 to 0.64 cm s$^{-1}$ at all the sites. And if the mass fraction of $PM_{10+}$ is larger than 20 %, the bulk $V_d$ for TSP could be higher than 1 cm s$^{-1}$ (size 9 and size 10). Apparently, a small percentage of $PM_{10+}$ mass contributed significantly to the bulk $V_d$ for TSP. A field study measuring metal dry fluxes using surrogate surfaces also suggested the important role of large particles contributing to the total fluxes (Zufall et al., 1998).

Due to the unavailability of the size distributions for metals measured in the present study, some assumptions were needed to calculate their $V_d$. Based on the sensitivity





ACPD
11, 32847–32875, 2011



tests presented in Table 3 and the review of size distributions presented in Sect. 3.1, size distributions as a combination of size 1, size 2 and size 3 were proposed for the several metals species (Table 2). It is noted that $V_d$ for a few species (Mn, Fe, Zn, and Cr) at Site V differ significantly from the other four sites; thus different size distributions for theses species at Site V were used (Table 2).

Modeled daily $V_d$ generally did not have any correlations with measured daily $V_d$ for most species and at most sites (figure not presented). This apparently should be due to the large uncertainties in the modeled $V_d$ due to various assumptions, large uncertainties in measured fluxes using surrogate surface, and some extent of uncertainties in measured concentrations, the latter two variables were used for obtaining measured $V_d$. However, annual average $V_d$ for all the species (except Pb) agreed very well with measured $V_d$ (e.g., only 10 % differences in many cases as shown in Fig. 4). For Pb, modeled $V_d$ were 30-50 % smaller then the measured values. If considering all the species together, modeled and measured annual $V_d$ values had a very good correlation (the last panel in Fig. 4).

While the assumed size distributions for most species can be easily justified based on previous measurements as reviewed in Sect. 3.1., we do not have much confidence for two species (Fe and Pb). As discussed in Sect. 3.1, the geometric mass median diameter (MMD) was largest for Fe and smallest for Pb; however, the measured $V_d$ in the present study had smallest values for Fe and largest values for Pb. For Fe, modeled $V_d$ can be made very close to the measured $V_d$ (as shown in Fig. 4) if the mass fraction of $PM_{10+}$ is limited to a very small percentage (e.g., 2 % or less) while assuming a large fraction of $PM_{2.5-10}$ (e.g., 80 % in Table 2) in order to satisfy the measured very large MMD values. However, it is difficult to obtain modeled $V_d$ as high as measured $V_d$ for Pb (as shown in Fig. 4) despite an assumption of 30 % mass fraction in $PM_{10+}$.

There were several possibilities causing the large differences in modeled and measured $V_d$ for Pb: (1) measured $V_d$ was overestimated using surrogate surface; (2) the MMD assumed for $PM_{2.5}$ fraction for Pb was too large (noting that $V_d$ increases with decrease in particle size for very small particles); (3) the modeled $V_d$ was underestimated





ACPD
11, 32847–32875, 2011



using daily averaged meteorological data (noting that daytime wind speed could be much higher then the daily average wind speed and that $V_d$ for small particles are more sensitive to wind speed). These factors can be identified in future studies with more accurate data of mass size fraction and meteorological variables.

### 3.3 Modeled fluxes and comparison with measurements

To support discussions presented in Sect. 2.5 above, correlations between modeled flux and measured concentrations were conducted (see one example shown in Fig. 5). As expected, modeled fluxes had good correlations with measured concentrations at all sites; the square of correlation coefficient was higher than 0.8 at two sites. Comparing values shown in Fig. 5 with those shown in Fig. 3, the correlations between modeled flux and measured concentrations were much better than those between measured fluxes and concentrations at four sites; the only exception is at Site IV for which the correlation actually declined. In general, modeled fluxes correlate reasonably well with measured concentration for all the species (figure not present).

Modeled and measured annual average fluxes and correlations between daily values of modeled and measured fluxes are presented in Table 4. Correlation coefficient ($R$), $F$ value (a test for statistical significance of the regression, obtained by dividing the explained variance by the unexplained variance) and the significance of the correlation $P(F)$ (the probability that the two group variables are not correlated) are shown in Table 4. If $F$ is smaller than 4.0 or $P(F)$ is larger than 0.1, the correlation will be considered insignificant. Only pairs satisfying both $F > 4.0$ and $P < 0.1$ are shown in the table.

Due to the very close $V_d$ values from model estimations and measurements as discussed in Sect. 3.2, modelled and measured annual average dry deposition fluxes were also very close, e.g., within 20 % at most cases for all metal species except Pb. Model estimated Pb fluxes were around 30 % lower than the measured fluxes.

Nearly 70 % of all the cases showed significant correlations between modelled and measured fluxes as shown in Table 4. This is surprising considering that there was





ACPD
11, 32847–32875, 2011



little correlation between modelled and measured $V_d$ values as discussed in Sect. 3.2. One reason for the significant correlation between modeled and measured fluxes could be because they both depended on measured concentrations. For example, Fe and Zn were two species whose measured fluxes correlated well with measured concentrations as discussed in Sect. 2.4. These two species were also found to have good correlations between modeled and measured fluxes (Table 4). Another example is Mn, which had much better correlation between measured fluxes and concentrations at Sites II to V than at Site I (Fig. 3); in comparison, correlations between modeled and measured fluxes at Sites II to V were also significant, but correlation was not found at Site I. Table 4 also shows that the worst performance was for Cu and As, which is consistent with the low correlations between measured fluxes and measured concentrations (Fig. S3). It is noticed that cases with (slightly) better correlations between measured fluxes and concentration do not always have better correlations between modeled and measured fluxes, and vice versa (compare species As at Site I with those at Sites II and III). The might be caused by uncertainties in modeled $V_d$ (and thus fluxes).

## 4 Conclusions

Measurements of daily air concentrations and dry deposition fluxes of seven metal species conducted at five sites in Central Taiwan during one year period and dry deposition velocities generated from these measurements were summarized in this study. Annual average concentrations were found to be the lowest in summer for all the seven species and at all the locations; however, the seasonal variations were generally small, e.g., mostly within a few ten percent. Highest concentrations appeared in different seasons for different species, but generally consistent from site to site due to the fact that the five sites are all within a small region of several hundred square kilometres. Annual average dry deposition fluxes were on the order of 3, 20, 400, 50, 25, 50 and 50 $\mu g\, m^{-2}\, day^{-1}$ for As, Mn, Fe, Zn, Cr, Cu and Pb, respectively. Seasonal variations in





ACPD
11, 32847–32875, 2011



deposition fluxes were mostly determined by those of air concentrations and to a less extent by those of deposition velocities. Geographical variations in deposition fluxes were smaller than those in air concentrations because the wetland site that had lowest air concentrations happened to have largest deposition velocities. The moderate to good correlations between measured fluxes and air concentrations for several species provided some confidence in the measured fluxes using surrogate surfaces; however, large uncertainties for several species at several sites might exist as seen from the lack of correlation between measured fluxes and concentrations.

Annual dry deposition velocities for the seven metal species ranged from 0.18 to 2.22 $cm\,s^{-1}$. These measured deposition velocities can be mainly reproduced using a size-segregated particle dry preposition model with assumed particle size distributions. However, modeled and measured daily deposition velocities had weak correlations despite their good agreement in annual average values. Sensitivity tests suggest that, for the several metal species considered in the present study, mass fraction of particles larger than 10 µm played a dominant role in the total deposition fluxes due to the much higher (e.g., by a factor of 20) deposition velocities of these large particles compared to those of fine ($PM_{2.5}$) and coarse ($PM_{2.5-10}$) particles. To estimate accurately the dry deposition fluxes of trace metals using inferential method, knowledge of the mass faction of $PM_{2.5}$, $PM_{2.5-10}$ and particles larger than 10 µm is required, if no detailed size distribution is available.

**Supplementary material related to this article is available online at: http://www.atmos-chem-phys-discuss.net/11/32847/2011/acpd-11-32847-2011-supplement.pdf**.





ACPD
11, 32847–32875, 2011



## References


Allen, A. G., Nemitz, E., Shia, J. P., Harrison, R. M., and Greenwood, J. C.: Size distributions of trace metals in atmospheric aerosols in the United Kingdom, Atmos. Environ., 35, 4581–4591, 2001.

Al-Momani, I. F., Momani, K. A., Jaradat, Q. M., Massadeh, A. M., Yousef, Y. A., and Alomary, A. A.: Atmospheric deposition of major and trace elements in Amman, Jordan, Environ. Monit. Assess., 136, 209–218, 2008.

Akhlaghi, Y. and Kompany-Zareh, M.: Comparing radial basis function and feed-forward neural networks assisted by linear discriminant or principal component analysis for simultaneous spectrophotometric quantification of mercury and copper, Anal. Chim. Acta, 537, 331–338, 2005.

Brüggemann, E., Gerwig, H., Gnauk, Th., Müller, K., and Herrmann, H.: Influence of seasons, air mass origin and day of the week on size-segregated chemical composition of aerosol particles at a kerbside, Atmos. Environ., 43, 2456–2463, 2009.

Chao, C. Y. and Wong, K. K.: Residential indoor $PM_{10}$ and $PM_{2.5}$ in Hong Kong and the elemental composition, Atmos. Environ., 36, 265–277, 2002.

Cho, S.-H., Richmond-Bryant, J., Thornburg, J., Portzer, J., Vanderpool, R., Cavender, K., and Rice, J: A literature review of concentrations and size distributions of ambient airborne Pb-containing particulate matter, Atmos. Environ., 45, 5005–5015, 2011.

de P. Pereira, P. A., Lopes, W. A., Carvalho, L. S., da Rocha, G. O., de Carvalho Bahia, N., Loyola, J., Quiterio, S. L., Escaleira, V., Arbilla, G., and de Andrade, J. B.: Atmospheric concentrations and dry deposition fluxes of particulate trace metals in Salvador, Bahia, Brazil, Atmos. Environ., 41, 7837–7850, 2007.

Fang, G. C., Wu, Y. S., Huang, S. H., and Rau, J. Y.: Dry deposition (downward, upward) concentration study of particulates and heavy metals during daytime, nighttime period at the traffic sampling site of Sha-Lu, Taiwan, Chemosphere, 56, 509–518, 2004.

Fang, G. C., Wu, Y. S., Chang, S. Y., Lin, J. B., and Lin, J. G.: Overall dry deposition velocities of trace elements measured at harbor and traffic site in Central Taiwan, Chemosphere, 67, 966–974, 2007a.

Fang, G. C., Wu, Y. S., Lee, W. J., Chou, T. Y., and Lin, I. C.: Ambient air particulates, metallic elements, dry deposition and concentrations at Taichung Airport, Taiwan, Atmos. Res., 84, 280–289, 2007b.






ACPD
11, 32847–32875, 2011



Flechard, C. R., Nemitz, E., Smith, R. I., Fowler, D., Vermeulen, A. T., Bleeker, A., Erisman, J. W., Simpson, D., Zhang, L., Tang, Y. S., and Sutton, M. A.: Dry deposition of reactive nitrogen to European ecosystems: a comparison of inferential models across the NitroEurope network, Atmos. Chem. Phys., 11, 2703–2728, doi:10.5194/acp-11-2703-2011, 2011.

Funasaka, K., Sakai, M., Shinya, M., Miyazaki, T., Kamiura, T., Kaneco, S., Ohta, K., and Fujita, T.: Size distribution and characteristics of atmospheric inorganic particles by regional comparative study in Urban Osaka, Jpn. Atmos. Environ., 37, 4597–4605, 2003.

Holsen, T. M. and Noll, K. E.: Dry deposition of atmospheric particles: application of current models to ambient data, Environ. Sci. Technol., 26, 1802–1814, 1992.

Kasahara, M., Park, J. H., and Yamamoto, K.: Characterization of atmospheric aerosols separated by particle size and water solubility using PIXE analysis, Nucl. Instrum. Meth. B, 109–110, 471–475, 1996.

Karanasiou, A. A., Sitaras, I. E., Siskos, P. A., and Eleftheriadis, K.: Size distribution and sources of trace metals and n-alkanes in the Athens urban aerosol during summer, Atmos. Environ., 41, 2368–2381, 2007.

Kim, K. H., Mishra, V. K., Kang, C. H., Choi, K. C., Kim, Y. J., and Kim, D. S.: The ionic compositions of fine and coarse particle fractions in the two urban areas of Korea, J. Environ. Manage., 78, 170–182, 2006.

Koçak, M., Kubilay, N., Herut, B., and Nimmo, M.: Dry atmospheric fluxes of trace metals (Al, Fe, Mn, Pb, Cd, Zn, Cu) over the Levantine Basin: a refined assessment, Atmos. Environ., 39, 7330–7341, 2005.

Loska, K. and Wiechuła, D.: Application of principal component analysis for the estimation of source of heavy metal contamination in surface sediments from the Rybnik Reservoir, Chemosphere, 51, 723–733, 2003.

Lu R., Turco, R. P., Stolzenbach, K., Friedlander, S. K., Xiong, C., Schiff, K., Tiefenthaler, L., and Wang, G.: Dry deposition of airborne trace metals on the Los Angeles Basin and adjacent coastal waters, J. Geophys. Res., 108(D2), 4074, doi:1029/2001JD001446, 2003.

Makkonen, U., Hellén, H., Anttila, P., and Ferm, M.: Size distribution and chemical composition of airborne particles in South-Eastern Finland during different seasons and wildfire episodes in 2006, Sci. Total Environ., 408, 644–651, 2010.

Migon, C., Journel, B., and Nicolas E.: Measurement of trace metal wet, dry and total atmospheric fluxes over the Ligurian Sea, Atmos. Environ., 31, 889–896, 1997.

Monarca, S., Crebelli, R., Feretti, D., Zanardini, A., Fuselli, S., Filini, L., Resola, S.,





ACPD
11, 32847–32875, 2011



Bonardelli, P. G., and Nardi, G.: Mutagens and carcinogens in size-classified air particulates of a Northern Italian town, Sci. Total Environ., 205, 137–144, 1997.
Napier, F., D'Arcy, B., and Jefferies, C.: A review of vehicle related metals and polycyclic aromatic hydrocarbons in the UK environment, Desalination, 226, 143–150, 2008.
Odabasi, M., Muezzinoglu, A., and Bozlaker, A.: Ambient concentrations and dry deposition fluxes of trace elements in Izmir, Turkey, Atmos. Environ., 36, 5841–5851, 2002.
Paode, R. D., Sofuoglu, S. C., Sivadechathep, J., Noll, K. E., Holsen, T. M., and Keeler, G. J.: Deposition fluxes and mass size distributions of Pb, Cu, and Zn measured in Southern Lake Michigan during AEOLOS. Environ. Sci. Technol., 32, 1629–1635, 1998.
Petroff, A. and Zhang, L.: Development and validation of a size-resolved particle dry deposition scheme for application in aerosol transport models, Geosci. Model Dev., 3, 753–769, doi:10.5194/gmd-3-753-2010, 2010.
Pirrone, N., Keeler, G. J., and Warner, P. O.: Trends of ambient concentrations and deposition fluxes of particulate trace metals in Detroit from 1982 to 1992, Sci. Total Environ., 162, 43–61, 1995.
Rojas, C. M., Injuk, J., and van Grieken, R. E.: Dry and wet deposiiton fluxes of Cd, Cu, Pb and Zn into the Southern Bright of the North Sea, Atmos. Environ., 27, 251–259, 1993.
Sabin, L. D., Lim, J. H., Stolzenbach, K. D., and Schiff, K. C.: Atmospheric dry deposition of trace metals in the coastal region of Los Angeles, California, USA, Environ. Toxicol. Chem., 25, 2334–2341, 2006.
Sakata, M. and Marumoto, K.: Dry deposition fluxes and deposition velocities of trace metals in the Tokyo metropolitan area measured with a water surface sampler, Environ. Sci. Technol., 38, 2190–2197, 2004.
Sakata, M., Marumoto, K., Narukawa, M., and Asakura, K.: Regional variations in wet and dry deposition fluxes of trace elements in Japan, Atmos. Environ., 40, 521–531, 2006.
Sakate, M., Tani, Y., and Takagi, T.: Wet and dry deposition fluxes of trace elements in Tokyo Bay, Atmos. Environ., 42, 5913–5922, 2008.
Samara, C. and Voutsa, D.: Size distribution of airborne particulate matter and associated heavy metals in the roadside environment, Chemosphere, 59, 1197–1206, 2005.
Schwede, D. B., Zhang, L., Vet, R., and Lear G.: An intercomparison of the deposition models used in the CASTNET and CAPMoN networks, Atmos. Environ., 45, 1337–1346, 2011.
Singh, M., Jaquesb, P. A., and Sioutas, C.: Size distribution and diurnal characteristics of particle-bound metals in source and receptor sites of the Los Angeles Basin, Atmos.





ACPD
11, 32847–32875, 2011



Environ., 36, 1675–1689, 2002.
Singh, K. P., Malik, A., and Sinha, S.: Water quality assessment and apportionment of pollution sources of Gomti river (India) using multivariate statistical techniques-a case study, Anal. Chim. Acta, 538, 355–374, 2005.
Sofuoglu, S. C., Paode, R. D., Sivadechathep, J., Noll, K. E., Holsen, T. M., and Keeler, G. J.: Dry deposition fluxes and atmospheric size distributions of mass, Al, and Mg measured in Southern Lake Michigan during AEOLOS, Aerosol Sci. Technol., 29, 281–293, 1998.
Tasdemir, Y. and Kural, C.: Atmospheric dry deposition fluxes of trace elements measured in Bursa, Turkey, Environ. Pollut., 138, 462–472, 2005.
Tasdemir, Y., Kural, C., Cindoruk, S. S., and Vardar, N.: Assessment of trace element concentrations and their estimated dry deposition fluxes in an urban atmosphere, Atmos. Res., 81, 17–35, 2006.
Turšič, J., Podkrajsek, B., Grgic, I., Ctyroky, P., Berner, A., Dusek, U., and Hitzenberger, R.: Chemical composition and hygroscopic properties of size-segregated aerosol particles collected at the Adriatic coast of Slovenia, Chemosphere, 63, 1193–1202, 2006.
Wang, X., Sato, T., and Xing, B.: Size distribution and anthropogenic sources apportionment of airborne trace metals in Kanazawa, Jpn. Chemosphere, 65, 2440–2448, 2006.
Wu, Y. S., Fang, G. C., Chen, J. C., Lin, C. P., Huang, S. H., Rau, J. Y. and Lin, J. G.: Ambient air particulate dry deposition, concentrations and metallic elements at Taichung Harbor near Taiwan Strait, Atmos. Res., 79, 52–66, 2006.
Wu, Y. S., Fang, G. C., and Lin, S. H.: Season variations for metallic elements compositions study in plant Bidenens pilosa L. var. radiate Sch. in Central Taiwan, Environ. Monit. Assess., 168, 255–267, 2010.
Yi, S. M., Shahin, U., Sivadechathep, J., Sofuoglu, S. C., and Holsen, T. M.: Overall elemental dry deposition velocities measured around Lake Michigan, Atmos. Environ., 35, 1133–1140, 2001.
Yi, S. M., Totten, L. A., Thota, S., Yan, S., Offenberg, J. H., Eisenreich, S. J., Garney, J., and Holsen, T. M.: Atmospheric dry deposition of trace elements measured around the urban and industrially impacted NY-NJ harbor, Atmos. Environ., 40, 6626–6637, 2006.
Zhang, L., Gong, S., Padro, J., and Barrie, L. A.: A size-segregated particle dry deposition scheme for an atmospheric aerosol module, Atmos. Environ., 35, 549–560, 2001.
Zhang, L., Brook, J. R., and Vet, R.: A revised parameterization for gaseous dry deposition in air-quality models, Atmos. Chem. Phys., 3, 2067–2082, doi:10.5194/acp-3-2067-2003,





ACPD
11, 32847–32875, 2011



2003.
Zota, A. R., Willis, R., Jim, R., Norris, G. A., Shine, J. P., Duvall, R. M., Schaider, L. A., and Spengler, J. D.: Impact of mine waste on airborne respirable particulates in Northeastern Oklahoma, United States, J. Air Waste Manage., 59, 1347–1357, 2009.
Zufall, M. J., Davidson, C. I., Caffrey, P. F., and Ondov, J. M.: Airborne concentrations and dry deposition fluxes of particulate species to surrogate surfaces deployed in Southern Lake Michigan, Environ. Sci. Technol., 32, 1623–1628, 1998.





ACPD
11, 32847–32875, 2011



**Table 1.** Annual average (±standard deviation) of measured concentration (ng m$^{-3}$), dry deposition (μg m$^{-2}$ day$^{-1}$) and dry deposition velocity (cm s$^{-1}$) for seven metal species (As, Mn, Fe, Zn, Cr, Cu and Pb) in total suspended particulates at five sites during September 2009 to August 2010.

| | Concentration (ng m$^{-3}$) | | | | | Flux (μg m$^{-2}$ day$^{-1}$) | | | | | Deposition velocity (cm s$^{-1}$) | | | | |
|---|---|---|---|---|---|---|---|---|---|---|---|---|---|---|---|
| | Site I | Site II | Site III | Site IV | Site V | Site I | Site II | Site III | Site IV | Site V | Site I | Site II | Site III | Site IV | Site V |
| As | 3.2±0.74 | 3.2±0.62 | 2.8±0.43 | 3.6±0.52 | 2.8±0.34 | 2.7±0.63 | 2.6±0.50 | 2.9±0.48 | 3.4±0.59 | 2.6±0.48 | 1.05±0.29 | 0.97±0.20 | 1.23±0.23 | 1.13±0.25 | 1.08±0.17 |
| Mn | 36±8.4 | 55±13.2 | 60±15.3 | 82±18.4 | 25±7.5 | 23±4.5 | 22±5.1 | 20±5.8 | 26±6.1 | 20±6.1 | 0.76±0.17 | 0.46±0.08 | 0.40±0.10 | 0.37±0.05 | 0.98±0.24 |
| Fe | 2548±960 | 2722±669 | 2408±657 | 2764±648 | 1898±571 | 419±84 | 420±90 | 423±86 | 436±109 | 412±120 | 0.22±0.11 | 0.18±0.03 | 0.22±0.08 | 0.19±0.05 | 0.26±0.04 |
| Zn | 104±31 | 90±21 | 94±25 | 109±26 | 69±20 | 49±10 | 50±12 | 50±13 | 51±16 | 49±15 | 0.58±0.14 | 0.65±0.09 | 0.63±0.12 | 0.56±0.17 | 0.85±0.14 |
| Cr | 24±6.9 | 33±7.2 | 245±8.2 | 32±6.9 | 18±5.9 | 25±6.4 | 25±6.4 | 25±6.9 | 27±6.1 | 24±8.3 | 1.32±0.48 | 0.93±0.32 | 1.35±0.59 | 1.01±0.29 | 1.60±0.59 |
| Cu | 90±27 | 71±20 | 79±22 | 110±53 | 61±17 | 57±16 | 47±19 | 52±22 | 66±18 | 44±17 | 0.81±0.35 | 0.84±0.4 | 0.82±0.36 | 0.78±0.34 | 0.88±0.35 |
| Pb | 34±13 | 29±13 | 32±14 | 39±11 | 25±11 | 55±13 | 45±15 | 51±18 | 61±17 | 44±17 | 2.08±0.80 | 2.07±1.1 | 2.07±1.10 | 1.88±0.56 | 2.22±1.09 |





ACPD
11, 32847–32875, 2011



**Table 2.** Different combinations of size 1, size 2 and size 3 (in percentage) for $V_d$ sensitivity tests (size 4 to size 10) and for $V_d$ and F calculations of seven metal species. size 1, size 2 and size 3 are three single lognormal size distribution representing $PM_{2.5}$, $PM_{2.5-10}$ and $PM_{10+}$, respectively, as shown in Fig. S4.

| | Size 4 | Size 5 | Size 6 | Size 7 | Size 8 | Size 9 | Size 10 |
|---|---|---|---|---|---|---|---|
| Size 1 | 80 | 50 | 20 | 80 | 50 | 40 | 30 |
| Size 2 | 20 | 50 | 80 | 10 | 40 | 40 | 40 |
| Size 3 | 0 | 0 | 0 | 10 | 10 | 20 | 30 |
| | For dry deposition calculation at all sites | | | | | | |
| | As | Mn | Fe | Zn | Cr | Cu | Pb |
| Size 1 | 40 | 50 | 20 | 50 | 30 | 45 | 40 |
| Size 2 | 40 | 40 | 80 | 40 | 50 | 40 | 30 |
| Size 3 | 20 | 10 | 0 | 10 | 20 | 15 | 30 |
| | For dry deposition calculation at Site V only | | | | | | |
| | | Mn | Fe | Zn | Cr | | |
| Size 1 | | 40 | 20 | 45 | 20 | | |
| Size 2 | | 40 | 78 | 40 | 50 | | |
| Size 3 | | 20 | 2 | 15 | 30 | | |





ACPD
11, 32847–32875, 2011



**Table 3.** Modeled deposition velocities (mean and standard deviation, $cm\,s^{-1}$) for 10 particle size distributions listed in Table 2 at the five sites.

| | | Size 1 | Size 2 | Size 3 | Size 4 | Size 5 | Size 6 | Size 7 | Size 8 | Size 9 | Size 10 |
|---|---|---|---|---|---|---|---|---|---|---|---|
| Site I | Mean | 0.12 | 0.20 | 3.75 | 0.14 | 0.16 | 0.18 | 0.49 | 0.51 | 0.88 | 1.24 |
| | Stdv | 0.04 | 0.01 | 0.34 | 0.04 | 0.03 | 0.02 | 0.07 | 0.06 | 0.09 | 0.12 |
| Site II | Mean | 0.14 | 0.20 | 3.96 | 0.15 | 0.17 | 0.19 | 0.53 | 0.55 | 0.93 | 1.31 |
| | Stdv | 0.05 | 0.02 | 0.56 | 0.05 | 0.04 | 0.02 | 0.10 | 0.09 | 0.14 | 0.19 |
| Site III | Mean | 0.19 | 0.22 | 4.58 | 0.20 | 0.21 | 0.22 | 0.64 | 0.64 | 1.08 | 1.52 |
| | Stdv | 0.07 | 0.03 | 0.93 | 0.06 | 0.05 | 0.04 | 0.15 | 0.14 | 0.23 | 0.31 |
| Site IV | Mean | 0.19 | 0.21 | 4.31 | 0.19 | 0.20 | 0.21 | 0.60 | 0.61 | 1.02 | 1.44 |
| | Stdv | 0.08 | 0.02 | 0.88 | 0.07 | 0.05 | 0.04 | 0.15 | 0.14 | 0.22 | 0.30 |
| Site V | Mean | 0.09 | 0.20 | 3.82 | 0.11 | 0.14 | 0.17 | 0.46 | 0.49 | 0.85 | 1.21 |
| | Stdv | 0.04 | 0.02 | 0.44 | 0.04 | 0.04 | 0.04 | 0.11 | 0.11 | 0.19 | 0.27 |





ACPD
11, 32847–32875, 2011



**Table 4.** Measured and modeled annual dry deposition fluxes ($\mu g\,m^{-2}\,day^{-1}$) and the regression analysis between modeled and measured values.

| | | As | Mn | Fe | Zn | Cr | Cu | Pb |
|---|---|---|---|---|---|---|---|---|
| Site I | Measured | 2.7 | 23.0 | 419 | 49.4 | 25.2 | 57.0 | 54.9 |
| | Modeled | 2.4 | 16.0 | 398 | 45.7 | 17.8 | 53.9 | 35.9 |
| | *R*-correlation | 0.31 | | 0.55 | 0.35 | 0.33 | | |
| | *F*-value | 6.4 | | 25.4 | 8.5 | 7.5 | | |
| | *P*(*F*) | 0.014 | | 4.6E−6 | 0.005 | 0.008 | | |
| Site II | Measured | 2.6 | 21.6 | 420 | 50.4 | 25.3 | 47.2 | 45.4 |
| | Modeled | 2.5 | 25.7 | 439 | 41.8 | 26.5 | 45.1 | 32.6 |
| | *R*-correlation | | 0.46 | 0.60 | 0.55 | | | 0.47 |
| | *F*-value | | 15.7 | 34.2 | 25.7 | | | 17.0 |
| | *P*(*F*) | | 0.0002 | 2.2E−7 | 4.2E−6 | | | 0.0001 |
| Site III | Measured | 2.9 | 20.3 | 423 | 50.3 | 24.8 | 52.4 | 50.5 |
| | Modeled | 2.6 | 32.8 | 442 | 51.5 | 21.7 | 58.1 | 41.7 |
| | *R*-correlation | | 0.39 | 0.25 | 0.53 | 0.32 | | 0.43 |
| | *F*-value | | 10.9 | 4.0 | 23.5 | 6.8 | | 13.3 |
| | *P*(*F*) | | 0.0017 | 0.05 | 9.1E−6 | 0.011 | | 0.0005 |
| Site IV | Measured | 3.4 | 26.1 | 436 | 51.0 | 26.9 | 65.5 | 61.2 |
| | Modeled | 3.1 | 42.7 | 494 | 57.0 | 28.2 | 76.9 | 48.1 |
| | *R*-correlation | | 0.52 | 0.39 | 0.39 | | | 0.27 |
| | *F*-value | | 22.5 | 10.6 | 10.8 | | | 4.7 |
| | *P*(*F*) | | 1.3E−5 | 0.0018 | 0.0017 | | | 0.034 |
| Site V | Measured | 2.6 | 20.0 | 412 | 49.1 | 24.0 | 43.8 | 44.4 |
| | Modeled | 2.1 | 18.6 | 405 | 40.8 | 19.8 | 36.1 | 26.7 |
| | *R*-correlation | 0.30 | 0.64 | 0.75 | 0.79 | 0.48 | | 0.54 |
| | *F*-value | 5.9 | 43.2 | 79.4 | 103 | 18.4 | | 24.8 |
| | *P*(*F*) | 0.018 | 1.3E−8 | 1.2E−12 | 1.E−14 | 6.6E−5 | | 5.5E−6 |





ACPD
11, 32847–32875, 2011



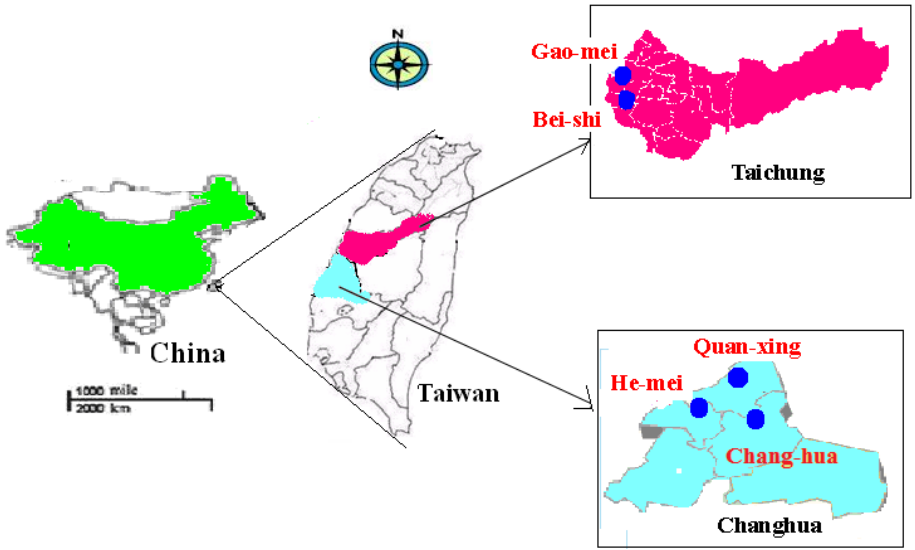


**Fig. 1.** Geographical location of the five sampling sites in Central Taiwan.





ACPD
11, 32847–32875, 2011



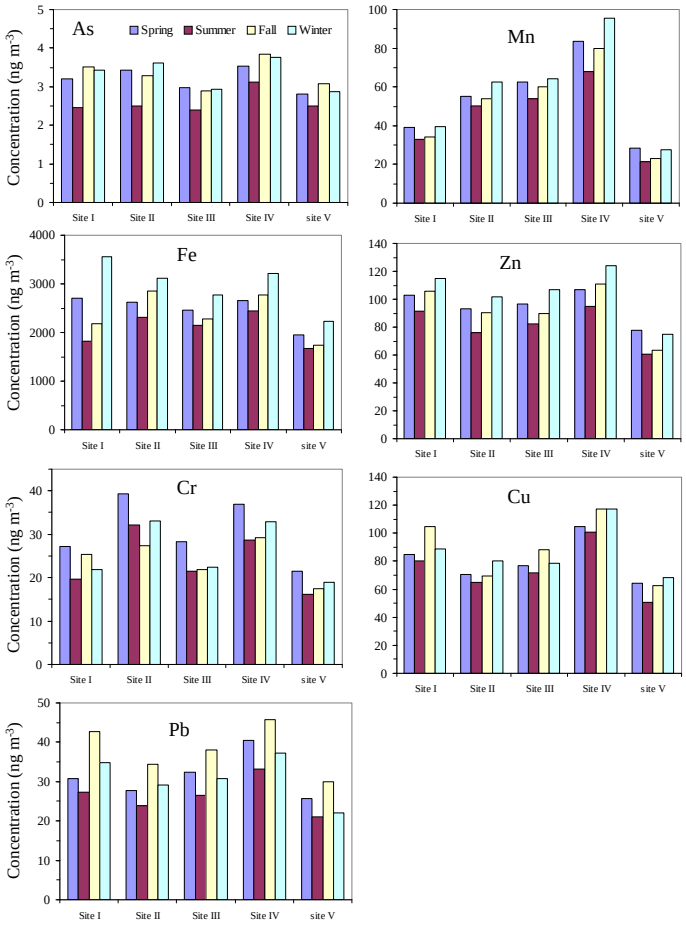


**Fig. 2.** Seasonal average concentration (ng m$^{-3}$) of As, Mn, Fe, Zn, Cr, Cu and Pb measured at the five sites.





ACPD
11, 32847–32875, 2011



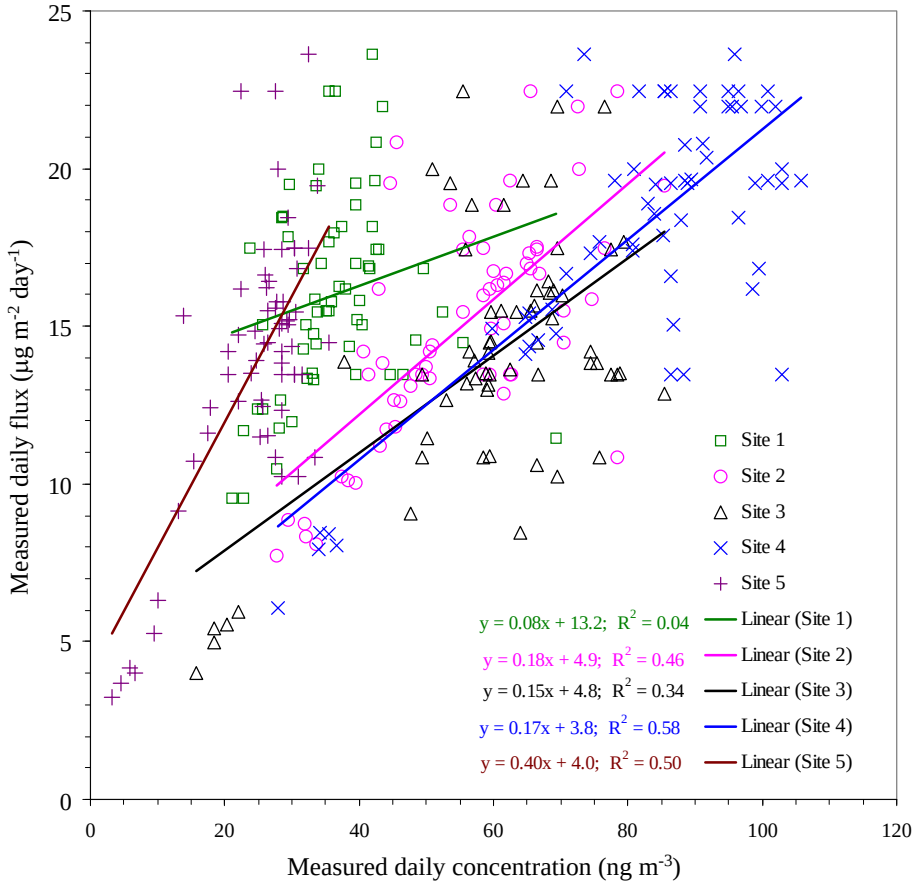


**Fig. 3.** Correlation between measured daily flux (μg m$^{-2}$ day$^{-1}$) and concentration (ng m$^{-3}$) for Mn at the five sites.





ACPD
11, 32847–32875, 2011



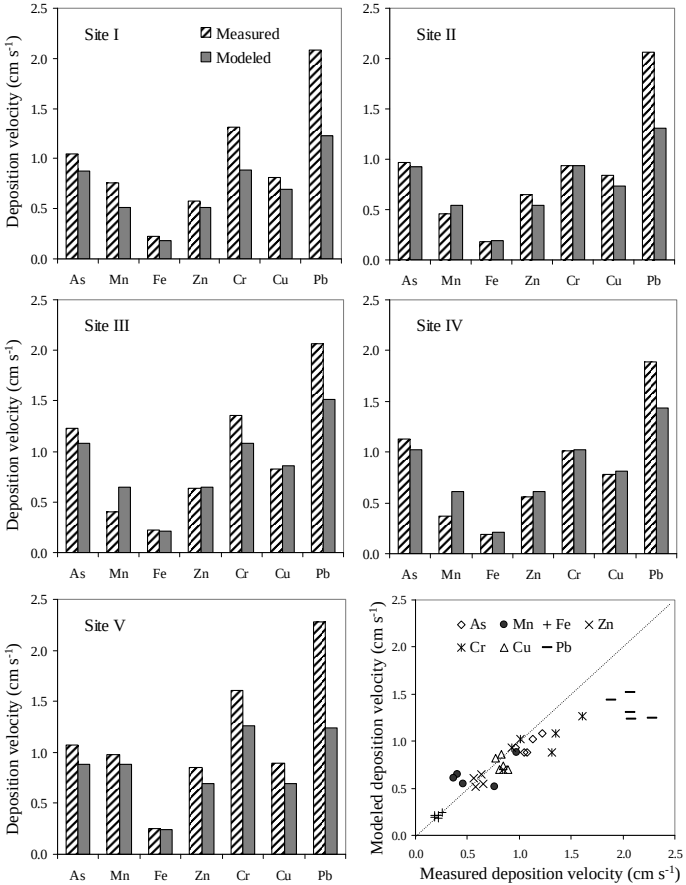


**Fig. 4.** Annual average of measured and modeled deposition velocity (cm $s^{-1}$) of As, Mn, Fe, Zn, Cr, Cu and Pb at the five sites and the scatter plot of these values.





ACPD
11, 32847–32875, 2011

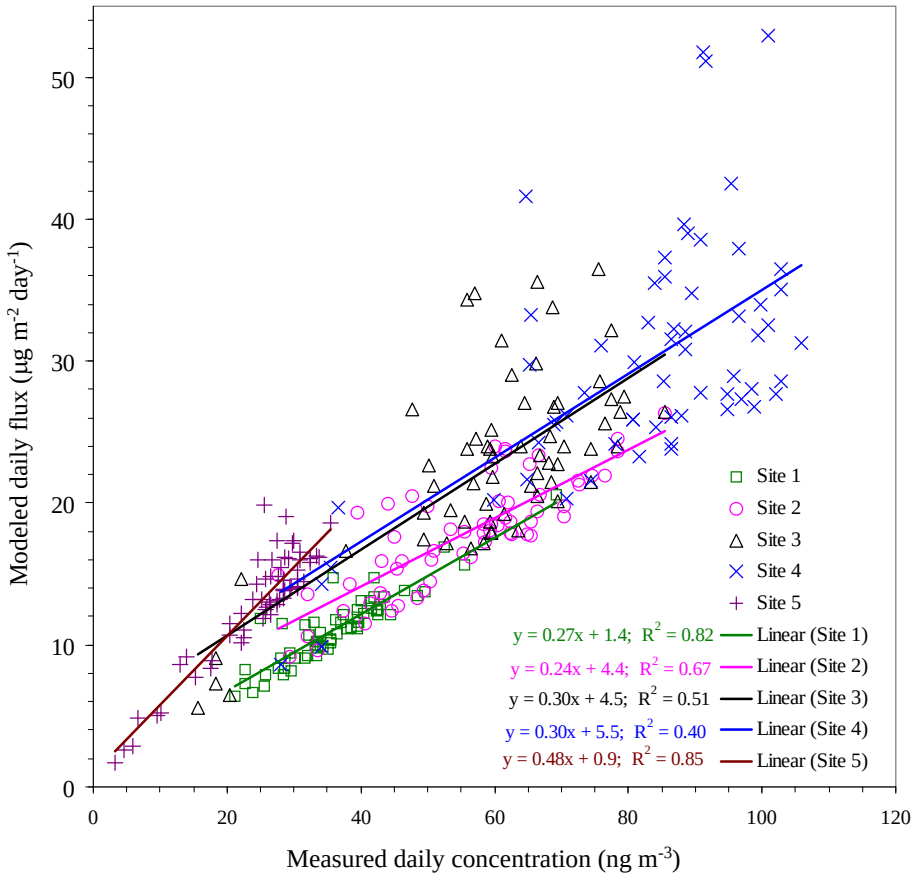


**Fig. 5.** Correlation between modeled daily flux (μg m$^{-2}$ day$^{-1}$) and measured daily concentration (ng m$^{-3}$) for Mn at the five sites.





ACPD
11, 32847–32875, 2011